Effect of Copper-Rich Regions on Tensile Properties of VPPA Weldments of 2219-T87 Aluminum

A copper-rich structure, appearing at the weld crown and root corners, has a detrimental effect on ductility and ultimate tensile strength

BY J. A. HARTMAN, R. J. BEIL AND G. T. HAHN

ABSTRACT. This study examines the relations between tensile properties and microstructural features of variable polarity plasma arc (VPPA) weldments of 2219-T87 aluminum. Crack initiation and weld failure of transverse tensile specimens of single and multipass weldments were studied. The specimens fractured on the rising portion of the stress-strain curve prior to necking, signifying that an increase in strength would accompany an increase in ductility.

Of particular interest is a shallow, typically 0.001–0.003-in. (0.03–0.08-mm) deep, copper-rich region located in the crown and root corners of the weld. This region is a primary source of crack initiation and growth, due to its brittle nature and highly strained location. The brittle regions were removed by electropolishing and machining to determine their effect on weld tensile properties. The removal increased the ductility of the weld specimens, and in the case of single pass welds, actually increased the load carrying capacity. Local strain measurements and metallographic and chemical analyses are presented.

KEY WORDS

Varib Polarity PAW
VPPA Aluminum Welds
VPPA Weld Properties
VPPA Weld Strength
Copper-Rich Region
Overlap Structures
Weld Brittle Regions
Weld Crack Initiatio
Weld Crack Growth
Plasma Welding

J. A. HARTMAN is with Advanced Composite Systems, Inland Division, GMC, Dayton, Ohio. R. J. BEIL is an Associate Professor of Engineering Mechanics, and G. T. HAHN is a Professor of Metallurgical Engineering, at Vanderbilt University, Nashville, Tenn.

Introduction

The load carrying capacity of fusion welded 2219-T87 aluminum depends on the weld geometry, the resistance to plastic flow, and the resistance to fracture (ductility). Figure 1 illustrates the role these elements play in the failure process of a single pass weld subjected to transverse tensile loading. The importance of the weld geometry is discussed by Nunes, Novak and McIlwain (Ref. 1). They present a soft interlayer theory for plastic flow, with the hard base material on either side of the softer (interlayer) weld material. The harder base material and the added bulk of the crown and root confine the majority of the plastic flow to diagonal paths, called crossover regions, across the soft weld metal—Fig. 1B.

The stress-strain characteristics of the weld—resistance to plastic flow—depend on the microstructure in the crossover region. However, the maximum load these welds can support depends on the ductility, *e.g.*, resistance to crack initiation and crack growth, because tensile specimens fail before

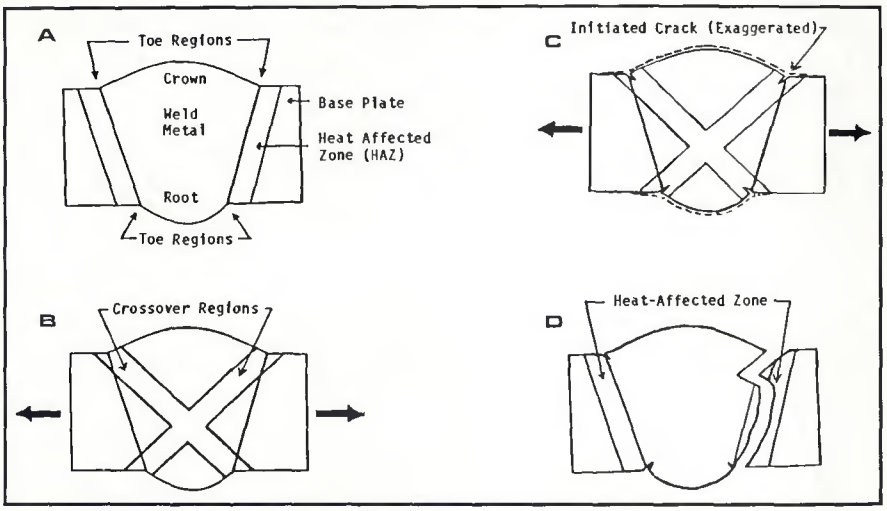

Fig. 1—Failure process of single pass weld. A—Schematic of the cross-section of a single pass VPPA butt weld of 2219-T87 aluminum; B—Under transverse tensile loading, the bulk of the plastic flow is confined to the diagonal crossover regions in the weld metal; C—Cracks initiate in the crown and root corners (toe regions) where a high-copper content coincides with the crossover regions; D—Specimen fails primarily along the heat-affected zone via ductile fracture

necking; *i.e.*, they fail while the stress-strain curve is still rising. In other words, the ultimate strength is limited by a fracture process rather than by a necking instability.

Previous work indicates that the fracture initiates in brittle regions at the crown and root corners of the welds—Fig. 1C (Refs. 2–4). D'Annessa (Ref. 5) identifies these brittle regions as massive secondary phase "overlap" structures that commonly occur during arc fusion welding of aluminum alloys. He illustrates their presence in 5456 GMA welds, and GTA welded 6061 and X7006 alloys, and also states that the regions are observed in 2219, 2014 and other X7000 alloy weldments. Burghard and Norris (Ref. 2) investigated GTA welds of 0.75-in. (19-mm)-thick 2219-T87 aluminum. They observed a needle-like precipitate in the weld toe regions, and tentatively identified it as beta phase (Al-Cu-Fe). By incremental loading of tensile specimens, they determined that crack initiation of the weld occurred in the brittle toe regions at 92–97% of the ultimate tensile stress. No cracking was found at the 0.2% offset yield stress. Van Dyke (Ref. 6) observed an agglomeration of brittle intermetallic ($CuAl_2$) constituents in the toe regions of VPPA welded 0.320-in (8-mm)-thick 2219-T87 aluminum, and related this to a premature cracking of the weld at these sites. Beil, Hartman and Hahn (Refs. 3, 4) have also found a brittle region in the root and crown corners of GTA welds and single and double pass VPPA welded 2219-T87 aluminum. At the surface, the brittle region exhibited a "cellular" structure. Chemical analyses of this region revealed copper contents in the range of 30–35 wt-% copper and 65–70 wt-% aluminum, thus indicating it is the eutectic mixture of $CuAl_2(\theta)+Al(\alpha)$. Their studies also confirm that the copper-rich cellular (CRC) region is a primary source of crack initiation, which subsequently leads to weld failure.

The research described here attempts to answer three questions. To what extent do these brittle regions exist in single and multipass VPPA welds? How much do these regions affect the ductility of the weld, and subsequently the load carrying capacity? Lastly, what is the origin of these regions?

The brittle region was removed by chemical or mechanical milling to determine its effect on tensile properties. Analysis of the results indicate that the CRC region is a limiting factor in weld ductility, particularly for single pass welds, whereby removal of the brittle region actually increases the load carrying capacity of the weld.

Experimental Materials and Methods

Tensile specimens were supplied by Martin Marietta Aerospace (Michoud Division, New Orleans) and NASA (Marshall Space Flight Center). Results for four different type butt welds of 2219-T87 aluminum plate are reported:

1. Single pass, VPPA, 2319 filler, 0.250-in. (6.4-mm)-thick plate.
2. Single pass, VPPA, 2319 filler, 0.375-in. (9.5-mm)-thick plate.
3. Double pass, VPPA, 2319 filler, 0.375-in. (9.5-mm)-thick plate.
4. Triple pass, VPPA, 2319 filler, 0.375-in. (9.5-mm)-thick plate.

The tensile specimens were cut transverse to the weld with the weld bead in the center, and were 11 in. (279 mm) long and either 1 or 2 in. (25 or 51 mm) wide. All specimens in this study were tested with the weld crown and root portions intact.

Nominal weight-percent chemical compositions of 2219 plate and 2319 filler wire are: Cu, 6.3%; Mn, 0.3%; V, 0.1%; Zr, 0.18%; Ti 0.06% (plate) and 0.15% (wire); and Al, the remainder. Specimens were polished by either mechanical or electrochemical means and etched with Keller's reagent. Weld bead surfaces and toe regions were electropolished according to ASTM Design E3-62 using the ratio for Class I-2 electrolyte at 10° to 15°C (50° to 59°F). Miccrostop was applied to surfaces where electropolishing was not desired. No etching was needed, but upon stopping the current flow, the specimen was left in the solution for about a minute to allow the built-up electrolytic film to dissipate from the specimen by magnetic stirring. This technique left what appeared to be a very thin coating of copper on the specimen.

Micrographs were made using a Hitachi X-650 microanalyzer (600-Å resolution), a hybrid scanning electron microscope, and a microprobe analyzer. Chemical analyses were performed using the PGT System 4 energy dispersive chemical analyzer, which has an accuracy of 1 at.-%.

Tensile tests were carried out on a Universal testing machine using a crosshead speed of 0.2 in. (5 mm) per minute. Prior to testing, the plate width, plate thickness, root width, crown width, and weld bead height were measured with a micrometer.

Yield stress (0.2% offset, 2-in. (51-mm) gauge length), ultimate stress, and load carrying capacity were calculated from load-elongation plots. Stress-strain curves were also calculated. Elongation measurements were derived from the displacement of 2-in. gauge marks after the test. Elongation values were also deduced from the load-time records of tensile tests. In some cases, the local strains were obtained from photodeposited grids (Ref. 7).

Experiments were conducted to (1) determine whether removal of the CRC region results in added tensile strength, (2) compare the strength of specimens where the CRC structure had been

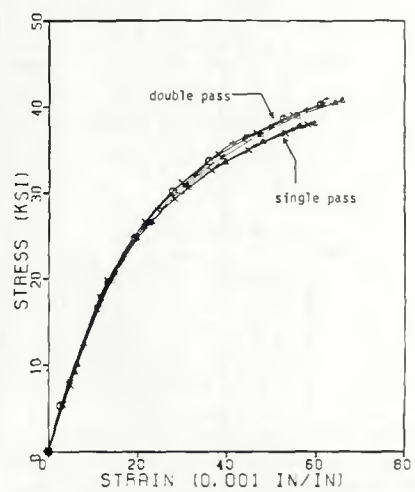

Fig. 2—Fracture strength, elongation and strain-hardening comparison of single pass VPPA welds with double pass VPPA welds

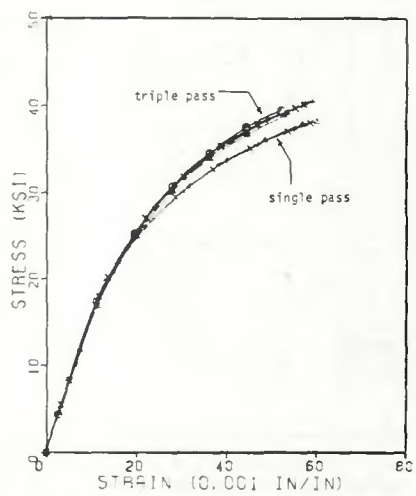

Fig. 3—Fracture strength, elongation and strain-hardening comparison of single pass VPPA welds with triple pass VPPA welds

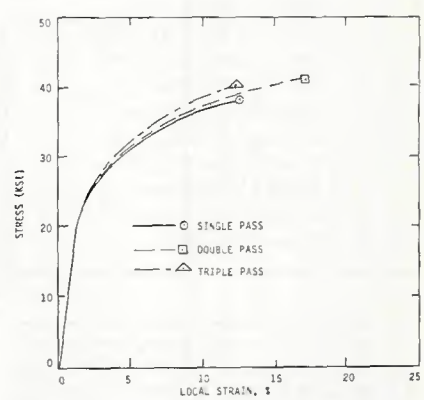

Fig. 4—Representation of the local stress-strain relationship at the point of fracture on the crown side of VPPA welded specimens

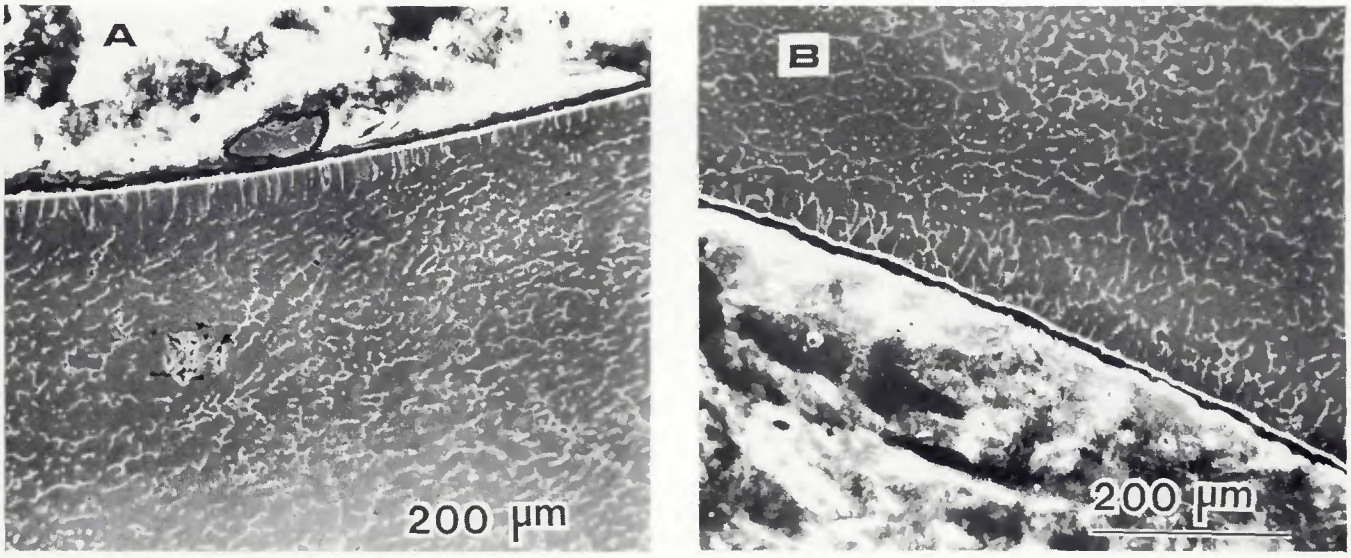

Fig. 5 — Cross-section of VPPA double pass weld showing CRC structure in weld toe regions. A — Crown; B — Root

removed from the toe regions of both the weld crown and root with the strength of specimens where removal was from the toe regions of the crown only, and (3) provide data for a statistical analysis from the limited number of specimens available.

For Experiment 1, specimens contained single or double pass butt welds of 0.25- or 0.375-in. thick 2219-T87 Al plate and were 1 or 2 in. wide. The samples were coated with Miccrostop except in the vicinity where they were to be polished, about 1 in. on either side of the weld. The CRC region was then removed by electropolishing for 90 min at a potential difference of 12 V. After testing, SEM examination of the weld cross-sections verified that the CRC region had been removed.

Specimens for Experiment 2 contained only double-pass welds on 0.375-in. plate and were 1 in. wide. Electrochemical removal was done by the same method as before. Mechanical milling was done using a 3/16-in. (5-mm) radius ball nose end mill cutting tool. Five mils (0.005 in.) were cut from the lowest side.

Eight specimens from each weld category (single pass, double pass, triple pass) were tested for Experiment 3. Four of each set of eight had the CRC region removed from both the crown and root toe regions. The method of removal in all cases was mechanical milling, done in the same manner as described earlier. The remaining four specimens from each category were tested in the as-welded condition. Based on the assumption that the specimens were numbered sequentially with respect to their relative positions on the welded plates from which test specimens were obtained, the following describes the specimen selection for this experiment.

1. Specimen Nos. 3–9 were alternately chosen for CRC region removal or to be tested as-welded. This was done to assure a "mixing" of tensile results in the event that the welding variables changed significantly down the length of the weld.

2. Specimen No. 15 from each category was tested to see if it would differ significantly from Specimens 4, 6 and 8, since supposedly it would be about 6–8 in. (152–203 mm) down-weld from No. 8.

Results

The following presents results for specimens tested in the as-welded condition. The stress-strain relationship was very reproducible within any weld category. The flow stress values at a particular strain for a single category were nearly identical, and in all cases, fracture occurred on the rising portion of the curve. However, the ductility values (elongation at fracture) often displayed a significant amount of variability within a category, *e.g.*, ±0.5%.

Stress-strain curves illustrating the differences in flow stress, strain hardening, and elongation between VPPA single pass, double pass, and triple pass welds are shown in Figs. 2 and 3. These curves show clearly the higher resistance to plastic flow of multipass welds as compared to single pass welds. The double pass welds had an average ductility of about 3.5%. The ductility of the triple pass weld was less than that of the double pass and roughly equal to that of the single pass, both being 2.8–3.0%. Resistance to plastic flow increased with increasing number of passes, whereas the ultimate strength was governed more by fracture characteristics.

In all cases, the measured strain was confined to a 2-in. gauge section. Figure 4 is a representation of the local stress-strain relationship at the point of fracture on the crown side of the single, double and triple pass weld specimens. The local fracture strain is computed as an average for the two specimens from each weld category (Ref. 7). The most prominent feature of Fig. 4 is that the local strain at the point of fracture is higher for double pass welds than for either single or triple pass welds. Thus, it is apparent for this limited number of samples that while the flow stress increases with increasing number of passes, a corresponding increase in ultimate strength is not realized, due to variations in ductility.

Samples from each weld category were examined to see if the CRC region was present in the weld corners. All welds inspected did exhibit the structure in both crown and root corners. The depth of the region is fairly consistent for weld specimens cut from the same test panel, but does vary from single pass to double pass, etc. It usually is about 1 to 3 mils deep (0.001–0.003 in.). A cross-section of a double pass weld shows the typical appearance of the structure in root and crown corners — Fig. 5. At the surface of the weld toe region, the structure exhibits a cellular appearance, with primary aluminum phase "cells" surrounded by the eutectic constituent — Fig. 6. Chemical analysis of this region shows the cells to have the following composition: 97 wt-% Al, 3 wt-% Cu. The matrix between the cells was found to contain: 63 wt-% Al, 37 wt-% Cu. The overall composition was 13 wt-% Cu, 87 wt-% Al. No significant amounts of impurities or trace elements were recorded.

In one instance, the structure of the brittle region took on a somewhat different appearance. Figure 7 is a cross-section of a triple pass specimen from the A series. In this series, the third pass lies

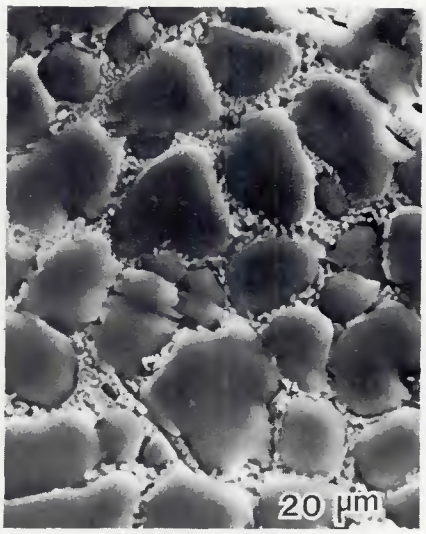

Fig. 6 — Cellular appearance of CRC regions at the surface of weld toe region

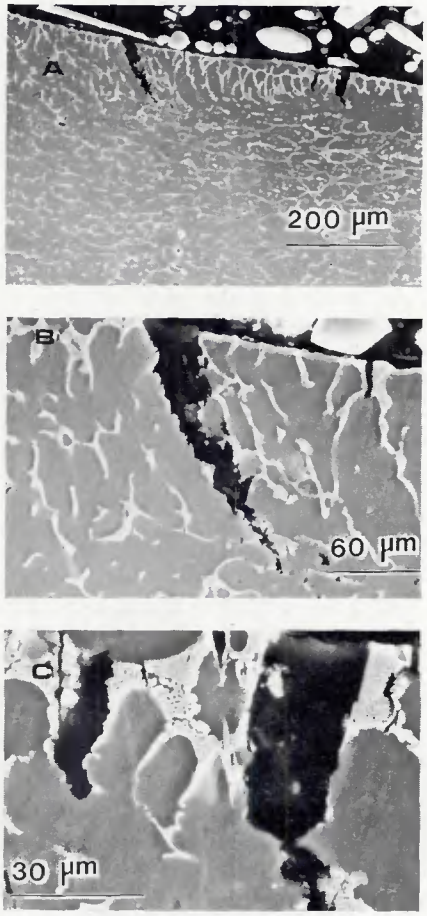

Fig. 9 — VPPA single pass weld tested to near failure. A — Cracks in the CRC region of crown corner; B — Higher magnification of A; C — Still higher magnification of A

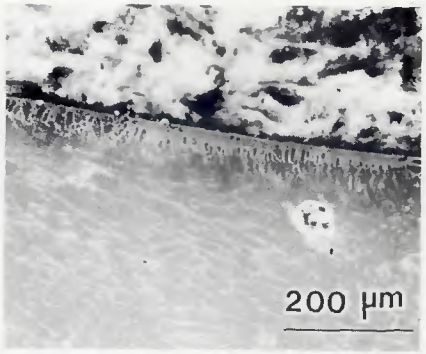

Fig. 7 — Cross-section showing the crown region of a VPPA triple pass weld, A series

within the borders of the second pass at the crown surface. The CRC structure at the surface extends from the edge of the third pass, down to the second pass and beyond. At one point, the structure becomes a fully eutectic surface layer, as can be seen in Fig. 8. Chemical analyses of this region show 64.0 wt-% Al, 36.0 wt-% Cu.

Samples from each category were studied to verify that crack initiation occurs in the weld toe regions prior to failure. Specimens were tensile loaded to near failure, unloaded, and examined. In each case, the root and crown corners were cracked in the CRC region. A typical cross-section shows initiated cracks in the crown corners of single pass VPPA welds — Fig. 9. A surface view of the root toe region of a single pass weld shows that the cracks proceed intergranularly within the CRC region either by eutectic debonding from the aluminum-rich cells or by eutectic cracking — Fig. 10. These initiated cracks were not observed at loads lower than approximately 90–95% of the weld's capacity.

The results from the three sets of removal experiments were as follows.

Experiment 1

After testing, SEM examination of cross-sections of the weld verified that the CRC structure had been removed. Tensile results are shown in Table 1. The increase in ultimate stress and elongation in each case is a sign that removal of the cellular region postpones the fracture process.

Experiment 2

An objective of Experiment 2 was to compare tensile properties of specimens with (a) CRC structure removed from crown only and (b) CRC structure removed from both root and crown.

The tensile results for these four specimens are shown in Table 2. These results and the consistency shown in the stress-strain curves (Fig. 11) indicate that the tested specimens had approximately the

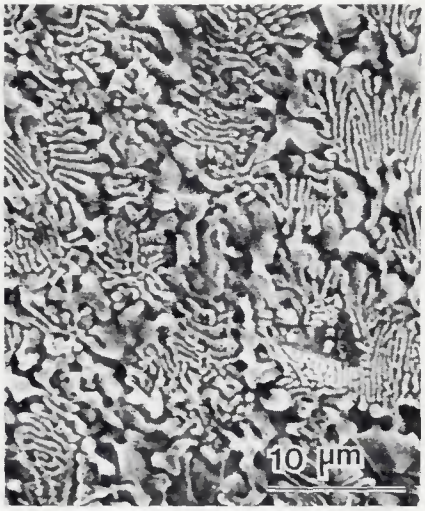

Fig. 8 — VPPA triple pass weld from A series. Surface view located between the second and third passes showing the continuous surface layer of eutectic

same elongation and fracture stress. The two different methods used to remove the CRC structure produced basically the same results. In these experiments, the double pass welds fracture outside the fusion zone in the base plate on the root side. Since the base material is tougher (harder) than the weld zone, it is unlikely that fracture initiation occurs on the root side in these cases.

Scanning electron micrographs of Specimen A2P7 (structure removed mechanically from crown only) reveal large amounts of eutectic in the region underneath the removed cellular structure. This region, after testing, exhibited extensive eutectic cracking and debonding, and was most likely the crack-initiating region — Fig. 12. Although no intensive quantitative studies have been done yet, possibly this region also has an excessive amount of copper (more than the 6.3% wt-% present in both plate and filler wire).

Experiment 3

Experiment 3 was designed as a statistical study of the effect of removal of the CRC region. Fracture load, or maximum load carrying capacity, was calculated from the load-elongation curves. Table 3 lists the fracture loads of these specimens.

For welds in the as-received condition, tensile tests show the following:

1. The double pass average fracture load was approximately 700 lb (5% or 1900 psi/13 MPa) higher than the single pass average fracture load.
2. The triple pass average fracture load was approximately 1000 lb (7% or 2700 psi/18.6 MPa) higher than the single pass average fracture load.

Removal of the CRC structure gave the

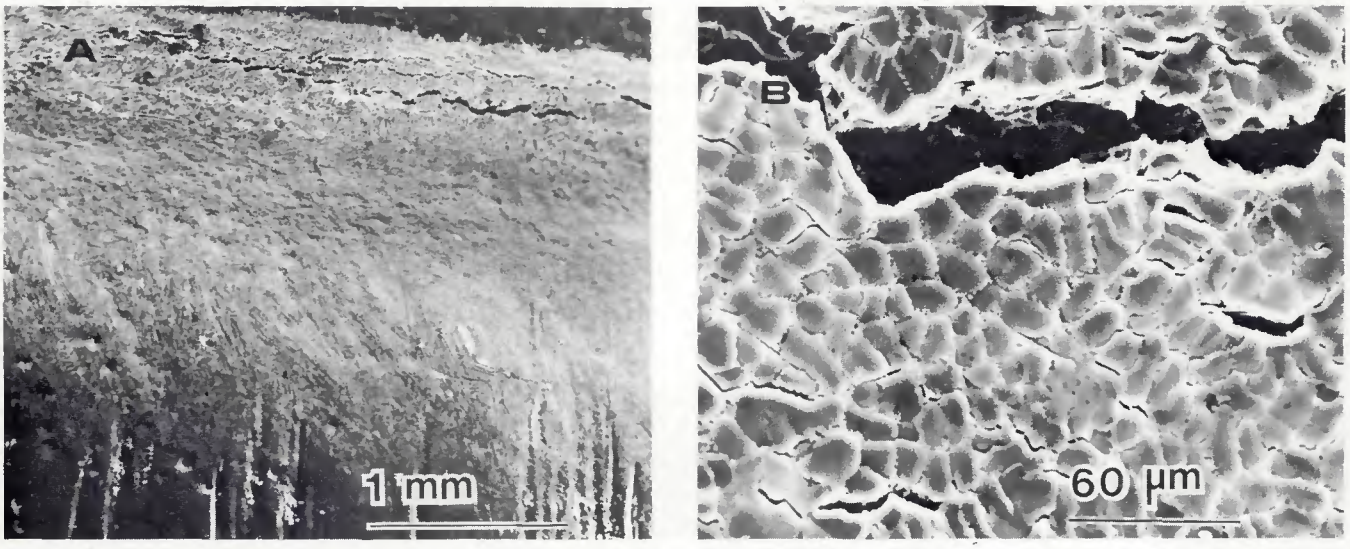

Fig. 10—VPPA single pass weld. A—Surface view of cracks in root toe region; B—Higher magnification of A, showing intergranular cracking of CRC region

following results:

1. Single pass—an increase in 3.75% (+528 lb) in the average fracture load was realized after CRC structure removal.

2. Double pass—a decrease of 1.1% (−162 lb) in the average fracture load was realized after CRC structure removal.

3. Triple pass—a slight increase of 0.5% (+72 lb) in the average fracture load was realized after CRC structure removal.

It is of particular interest to note that removal of the CRC region from the first pass increased its fracture load to within 1.3% of the as-received double pass specimens.

Considering average fracture load values, the results show that a second pass is slightly more effective in increasing the fracture load than removing the CRC structure from single pass welds.

Tables 4–6 list the tensile properties of specimens tested in Experiment 3, including fracture stress and measured elongation. Comparison of the stress-strain curves in the same weld-pass category for specimens as-received with specimens with the CRC structure removed shows a slight increase in strain-hardening, possibly due to cold work of machining. The curves also reveal an increase in elongation with CRC structure removal, except in the double pass category, thus indicating an increased resistance to crack initiation and propagation.

Table 7 lists the results of a statistical analysis of fracture strengths obtained during the CRC structure removal study. It shows that a significant improvement in fracture stress is gained by removing the CRC structure from VPPA single pass welds. Approximately 95% of such welds, when tested with cellular structure removed, should have higher fracture strength than those tested as-received (with CRC structure in the weld corners). Table 7 shows that there is no significant difference in fracture strength of VPPA double pass welds when tested as-received or with CRC structure removed, although there is a slight increase in average fracture stress. Table 7 also shows some improvement in the fracture stress of VPPA triple pass welds by removing the CRC structure. Fracture strength of Specimen 15 from each category was near to one standard deviation from the average fracture stress, a variation which is not considered significant. Figures 13A and 13B, stress-strain curves for single pass specimens, again show consistency of flow in this weld category. Some increase in elongation accompanies the

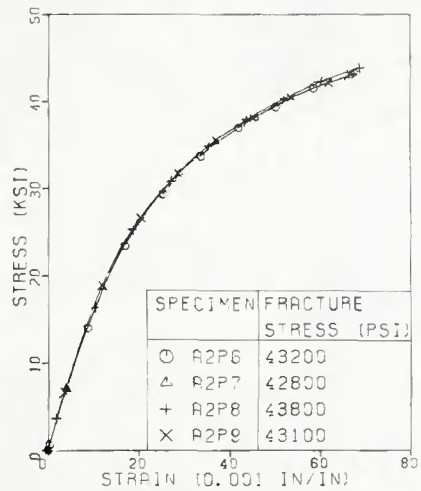

Fig. 11—Stress-strain curves for double pass VPPA butt welded 2219-T87 Al 0.375-in.-thick plate. CRC structure removed in crown and root corners of A2P6 and A2P9. CRC structure removed crown corners only on A2P7 and A2P8

Table 1—Comparison of Tensile Properties for Specimens As-Received vs. Specimens Electropolished (Before Testing) to Remove Crack Initiation Sites (CRC Structure) at the Weld Corners

Specimen	Width (in.)	Condition of Cellular Structure	Yield Stress 0.2% Offset, 2-in. Gauge (psi)[a]	Ultimate Stress (psi)[a]	Change in Ultimate Stress (psi)[a]	Measured Elongation (in.)	Change in Elongation (in.)
			Single Pass VPPA Weld				
720-12	1	intact	24500	40700	+2600		
720-3[b]	1	removed	23500	43300			
720-15	2	intact	18100	40200	+2300	0.082	
720-14	2	removed	19000	42500		0.094	+0.012
			Double Pass VPPA Weld				
654-3	1	intact	22000	42600	+2000		
655-4	1	removed	21300	44600			
654-6	2	intact	18400	43000	+2000	0.119	
655-7	2	removed	20900	45000		0.132	+0.13

[a]Note: All stress values rounded to nearest 100 psi.
[b]Specimen unloaded during test, removed for measurements, and then tensile tested to fracture.

Table 2—Tensile Properties of Double Pass, 2319 Filler VPPA Specimens with CRC Regions Either Partially (Crown Only) or Totally (Both Crown and Root) Removed

Specimen	Condition of Cellular Region	Yield Stress (psi)	Ultimate Stress (psi)	Measured Elongation, 2-in. Gauge (%) Average Crown and Root	Crown Width (in.)	Root Width (in.)	Plate Width (in.)	Plate Thickness (in.)
A2P6	Removed mechanically from both crown and root	19200	43200	5.7	0.557	0.344	0.956	0.372
A2P7	Removed mechanically from crown only	20600	42800	5.2	0.570	0.326	0.961	0.375
A2P8	Removed electrochemically from crown only	19200	43800	5.5	0.488	0.314	0.957	0.366
A2P9	Removed electrochemically from both crown and root	20000	43100	6.0	0.491	0.316	0.941	0.364

Table 3—Fracture Loads (lb) of Specimens Tested in the CRC Structure Removal Study

Testing Condition	Specimen Number	B1P	B2P	B3P
As-welded	4	14000	14700	15000
	6	13700	14900	14800
	8	13900	14900	15100
	15	14500	14400	15200
Cellular structure removed	3	14300	14900	14700
	5	14600	14700	15200
	7	14600	14600	15300
	9	14700	14200	15200

increase in fracture stress.

Figure 14, weld cross-sections of both tested and untested specimens, shows the failure paths for the various welds. Double pass and triple pass VPPA welds fail generally in the same manner. Crack initiation takes place in the crown corner; the fracture path follows the fusion line of the second pass; upon reaching the interface between the first and second passes, the fracture follows the heat-affected zone of the first pass for a distance, then ends in the base plate on the root side of the weld. As the base metal is harder and also more crack resistant, it follows that for double and triple pass welds, the critical crack leading to failure is most likely initiated in the crown corner, and not the root corner or adjacent base metal.

Figure 15 illustrates the fracture at the crown corner of double and triple pass VPPA welds tested as-received. The point of fracture at the crown of the double pass is associated with a very thin layer of brittle copper; in fact, the fracture lies almost, if not completely, outside the copper-rich region. On the other hand, the point of fracture at the crown corner of the triple pass weld is in the midst of the CRC region.

Removal of the CRC region did not alter the fracture path of double and triple pass welds. Also, as mentioned previously, the tensile properties were not changed significantly by removing the CRC region. This suggests that the brittle region may not always be a major factor in the strength and ductility of double and triple pass welds.

The crack growth in single pass welds

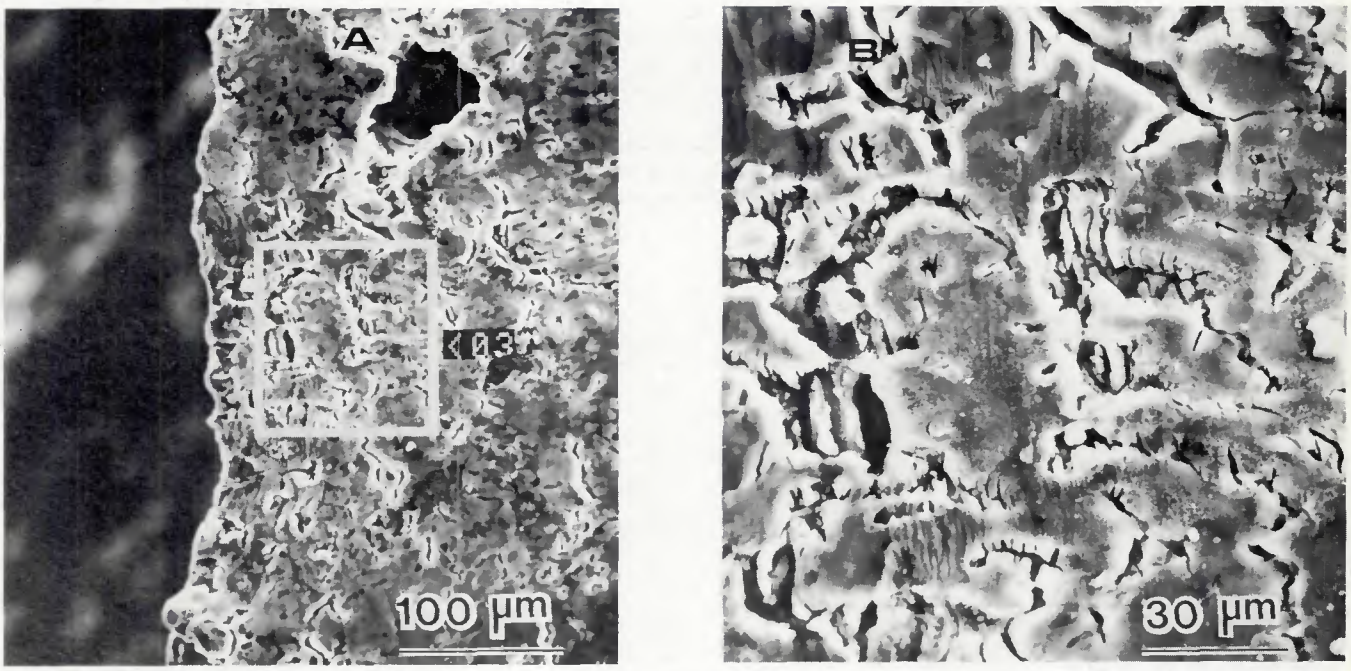

Fig. 12—A—Specimen A2P7, surface view of fracture site in crown corner; B—Higher magnification of A shows excessive eutectic cracking and debonding

Table 4—Comparison of Tensile Properties for Single Pass VPPA 2219-T87 Aluminum Welds Tested As-Received and after Removal of CRC Structure

Specimen	Testing Condition	Yield Stress (psi) 0.2% Offset, 2-in. Gauge	Ultimate Stress (psi)	Measured Elongation, 2-in. Gauge (%)	Crown Width (in.)	Root Width (in.)	Crown to Root Thickness (in.)	Plate Width (in.)	Plate Thickness (in.)
B1P4	As-welded	20200	39000	4.6	0.549	0.316	0.509	0.960	0.374
B1P6		20500	38200	4.2	0.573	0.323	0.515	0.957	0.374
B1P8		20700	38700	4.3	0.556	0.314	0.505	0.959	0.374
B1P15		19100	40400	5.0	0.542	0.356	0.515	0.960	0.374
B1P3	CRC region removed	21200	41400	6.1	0.505	0.252	0.506	0.957	0.360
B1P5	mechanically from both	20500	42100	5.4	0.535	0.333	0.507	0.959	0.361
B1P7	crown and root	20000	42300	5.7	0.545	0.323	0.506	0.959	0.360
B1P9		20700	42400	6.3	0.536	0.314	0.509	0.960	0.362

is not as readily determined as it is for double and triple pass welds. As seen in Fig. 14, the fracture path both starts and terminates in the weld corners. Closer examination reveals that the CRC structure is associated with the fracture path in both the crown and root corners—Fig. 16. Removal of the brittle region from single pass welds did alter the crack growth and fracture path—Fig. 17. Specimen B1P3 failed across the weld, from one weld corner to the diagonally opposite weld corner. Specimen B1P5 failed in the heat-affected zone, with the fracture initiating and terminating in the weld corners.

Specimens B1P7 and B1P9 fractured in a manner similar to as-received single pass welds (brittle region intact), but with the diagonal portion of the fracture entering into the root side of the weld (in contrast with the crown side in as-received specimens—Fig. 18). It appears that with this limited number of samples, removal of the CRC region from single pass welds alters not only the amount of stress required for crack initiation and extension, but also changes the path of fracture. These factors apparently explain the increases in the ductility, the ultimate strength, and the load carrying capacity of single pass welds lacking the CRC regions in the weld toes.

Figure 18 illustrates the typical fracture path of a single pass weld specimen that was tensile tested in the as-received condition. In the upper right-hand corner, one can see the portion of the fracture path that was directed across the weld towards the diagonally opposite root corner, in accordance with Fig. 1. Closer examination of the "crack tip"—where the fracture path changes course—reveals a series of microvoids that have initiated at second phase particles—Fig. 19. This line of microvoids continues towards the diagonally opposite root corner.

Table 5—Comparison of Tensile Properties for Double Pass VPPA 2219-T87 Aluminum Welds Tested As-Received and After Removal of CRC Structure

Specimen	Testing Condition	Yield Stress (psi) 0.2% Offset, 2-in. Gauge	Ultimate Stress (psi)	Measured Elongation, 2-in. Gauge (%)	Crown Width (in.)	Root Width (in.)	Crown to Root Thickness (in.)	Plate Width (in.)	Plate Thickness (in.)
B2P4	As-welded	19500	41200	4.5	0.546	0.335	0.502	0.958	0.373
B2P6		18400	41700	4.4	0.566	0.303	0.536	0.960	0.373
B2P8		19600	41600	5.0	0.572	0.311	0.528	0.960	0.373
B2P15		18000	40000	4.6	0.536	0.290	0.522	0.956	0.377
B2P3	CRC region removed	19500	43100	5.1	0.459	0.315	0.517	0.957	0.361
B2P5	mechanically from both	19500	42500	5.4	0.541	0.290	0.542	0.957	0.361
B2P7	crown and root	19100	42200	4.6	0.557	0.320	0.525	0.959	0.360
B2P9		19600	41100	5.0	0.554	0.328	0.509	0.958	0.360

Table 6—Comparison of Tensile Properties for Triple Pass VPPA 2219-T87 Aluminum Welds Tested As-Received and After Removal of CRC Structure

Specimen	Testing Condition	Yield Stress (psi) 0.2% Offset, 2-in. Gauge	Ultimate Stress (psi)	Measured Elongation 2-in. Gauge (%)	Crown Width (in.)	Root Width (in.)	Crown to Root Thickness (in.)	Plate Width (in.)	Plate Thickness (in.)
B3P4	As-welded	19400	41700	4.7	0.525	0.288	0.542	0.959	0.375
B3P6		20300	41000	4.7	0.547	0.323	0.541	0.960	0.375
B3P8		18700	42100	5.6	0.547	0.297	0.542	0.956	0.376
B3P15		18700	42300	6.2	0.555	0.320	0.543	0.959	0.374
B3P3	CRC region removed	21900	42500	4.6	0.544	0.303	0.541	0.958	0.361
B3P5	mechanically from both	20400	43800	5.4	0.545	0.315	0.545	0.962	0.361
B3P7	crown and root	20600	44400	4.8	0.516	0.309	0.542	0.956	0.360
B3P9		19500	44000	5.4	0.543	0.296	0.542	0.956	0.361

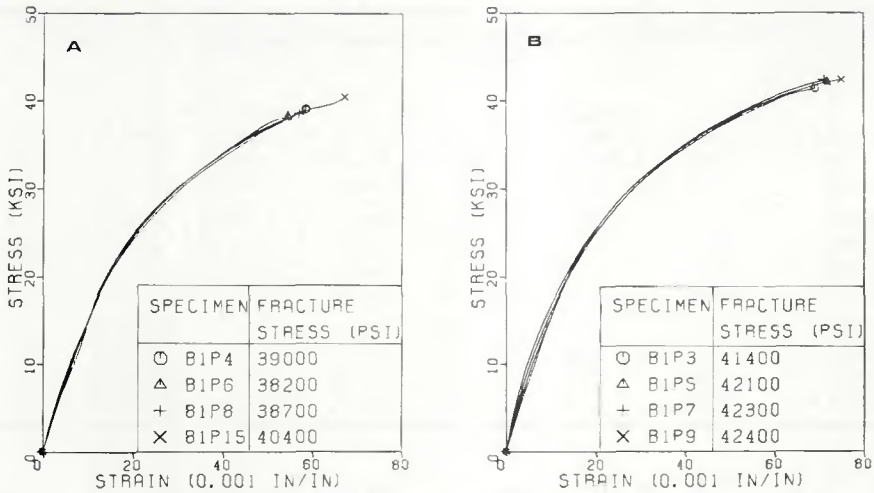

Fig. 13 — Stress-strain curves of single pass weld specimens tested. A — As-welded; B — After removal of CRC structure

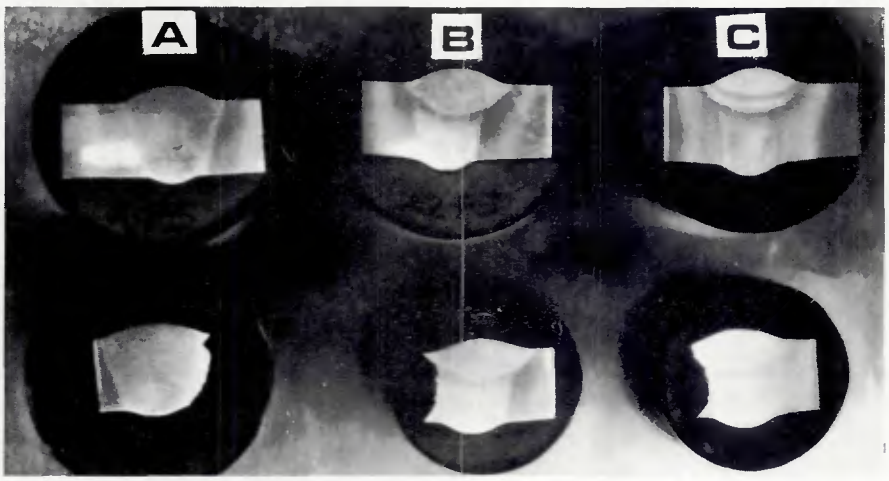

Fig. 14 — Photographs of polished and etched cross-sections of welds. A — Single pass VPPA, A series; B — Double pass VPPA, A series; C — Triple pass VPPA, A series

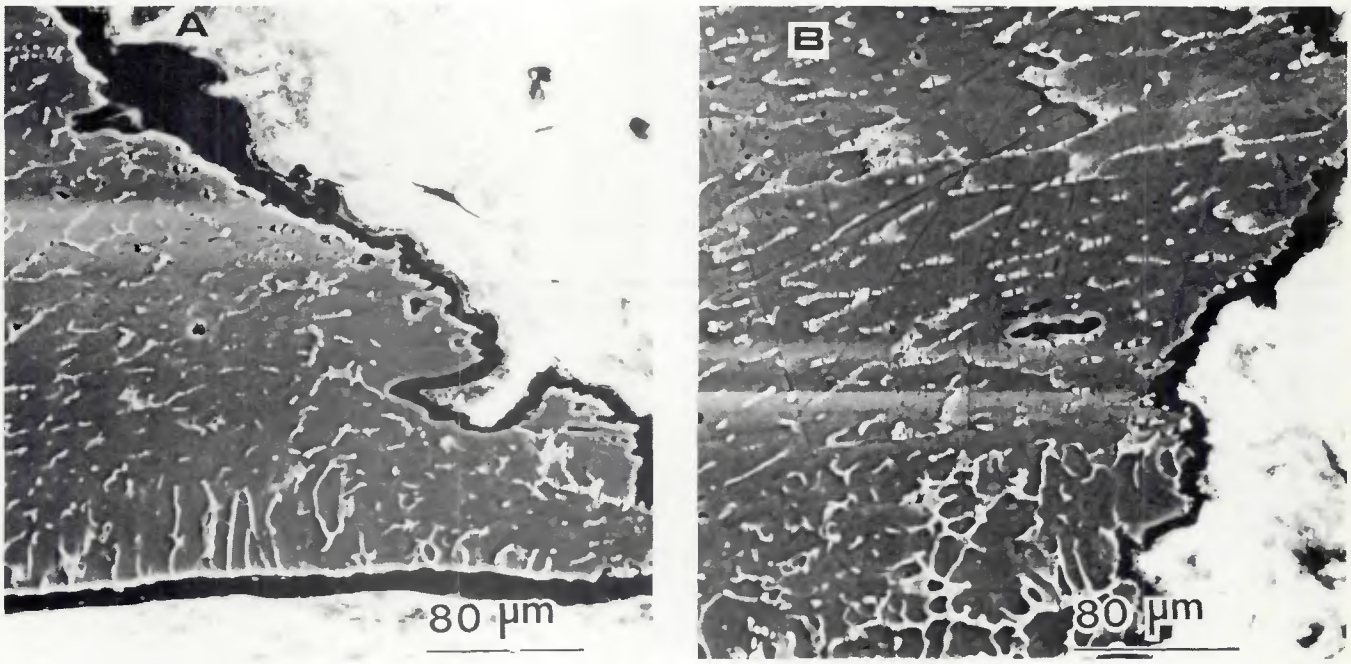

Fig. 15 — Fracture at crown corner of VPPA welds. A — Double pass weld; B — Triple pass weld

Discussion of Results

The local strain measurements show that the peak strains are produced at the crown and root corners. In agreement with Nunes interlayer theory (Ref. 1), this is where the crossover regions reach the surface, confining the majority of the plastic flow to the corners. Figure 19 is also supportive of the interlayer theory. The line of voids, caused by extensive plastic flow, is directed towards the diagonally opposite root corner, lying within the proposed crossover regions. This figure indicates that the crack growth process is one of nucleation, growth and coalescence of microvoids initiated at second phase particles, which is typical of ductile fracture. Burghard and Norris (Ref. 2) made similar conclusions from fractographic studies of GTA-welded 2219-T87 aluminum.

An important feature of the tensile properties of 2219-T87 aluminum fusion weldments is that the test specimens fail on the rising portion of the stress-strain curve by fracturing prior to necking. This shows that while the flow strength (*i.e.*, the stress at a particular plastic strain) expresses the weldment's resistance to plastic deformation, both the flow strength and the ductility of the weld determine the ultimate load it can carry. The ductility (or percent elongation), being the average strain at fracture of a 2-in. gauge section encompassing the weldment, is viewed as an integrated measure of the weld's resistance to crack initiation, stable growth, and crack extension. The ability of a tensile specimen to defer fracture enables it to continue to strain-harden, thereby permitting the

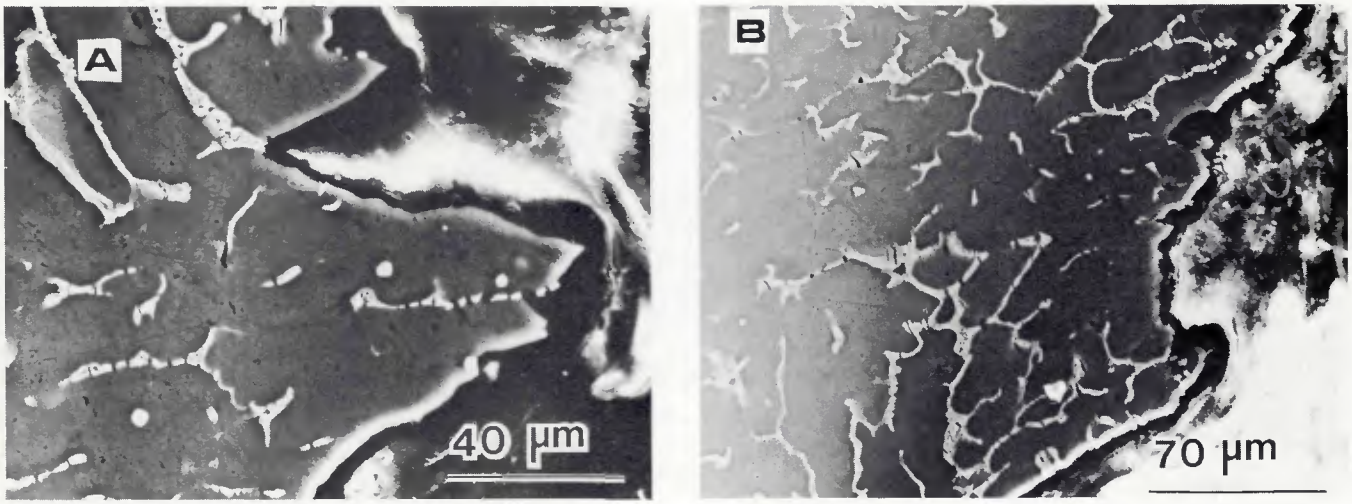

Fig. 16 — Points of crack initiation and fracture, VPPA single pass weld. A — Crown; B — Root

stress-strain curve to rise further. Thus, a one percentage point increase in the ductility (in the range from 2 to 5%) increases the ultimate strength of the welds by about 2000 psi (13.8 MPa).

The ductility, and therefore the strength, of these welds is limited by the brittle, high-copper regions in the weld corners. Present in all welds inspected, the CRC regions are a primary site of crack initiation and premature weld failure. This work shows that removal of CRC structure from the specimens in the B series had relatively little effect on the ultimate tensile strength of the double pass welds, the 2.7% increase coming from a similar increase in flow stress. The ultimate tensile strength of the single pass welds and the triple pass welds were significantly increased, largely due to increases of 31% and 13%, respectively, in elongation, with an accompanying increase of 3% and 4%, respectively, in flow stress — Table 8. In the case of the single pass 2319-filler-VPPA weld, the removal of material from the cross-section actually increased the load carrying capacity. Further evidence comes from the observation that in the A series for specimens tested as-received, the higher ductility of the double pass relative to the single pass and triple pass weld (4% compared to 3.5%) is connected with a very shallow CRC region in the double pass weld where the crossover region comes to the surface. This observation suggests that one of the benefits of the second pass is to place the CRC region in a less sensitive location relative to the crossover region. Another possibility is that the critical crack leading to failure initiates in the root of single pass specimens and that removal of it alone (without removing material from the crown) may give an increase in ductility and load carrying capacity. Experiments need to be done to verify this possibility.

The origin of the high-copper region in the weld corners is not clear. The substitution of non-copper-based 4043 wire did not prevent the occurrence of the CRC region (Ref. 7); apparently, the filler metal does not play a major role in the segregation mechanism. This is also suggested by the fact that the triple pass welds studied (wherein the third pass is a heat pass and uses no filler wire) also have the brittle high-copper region associated at the edges of the third pass. As mentioned previously, D'Annessa discusses the occurrence of these secondary phase overlap structures in GMA and GTA welds of 5456 (Al-Mg) 6061 (Al-Mg) and X7006 (Al-Zn-Mg), and states that they are also present in 2219, 2014 and other X7000 weldments. These structures

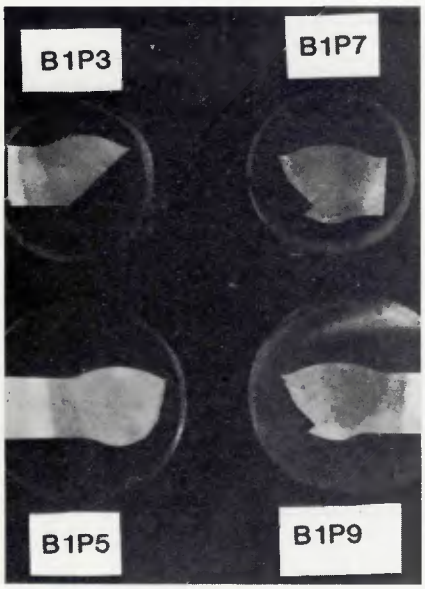

Fig. 17 — Cross-sections of fractured single pass welds tested with CRC structure removed

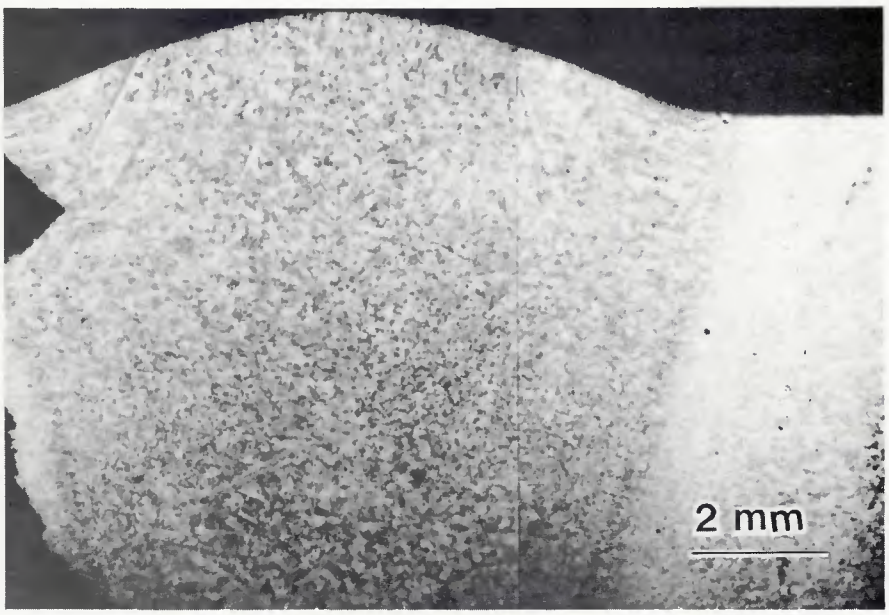

Fig. 18 — Cross-section of Specimen B1P2, single pass VPPA weld, tested as-received

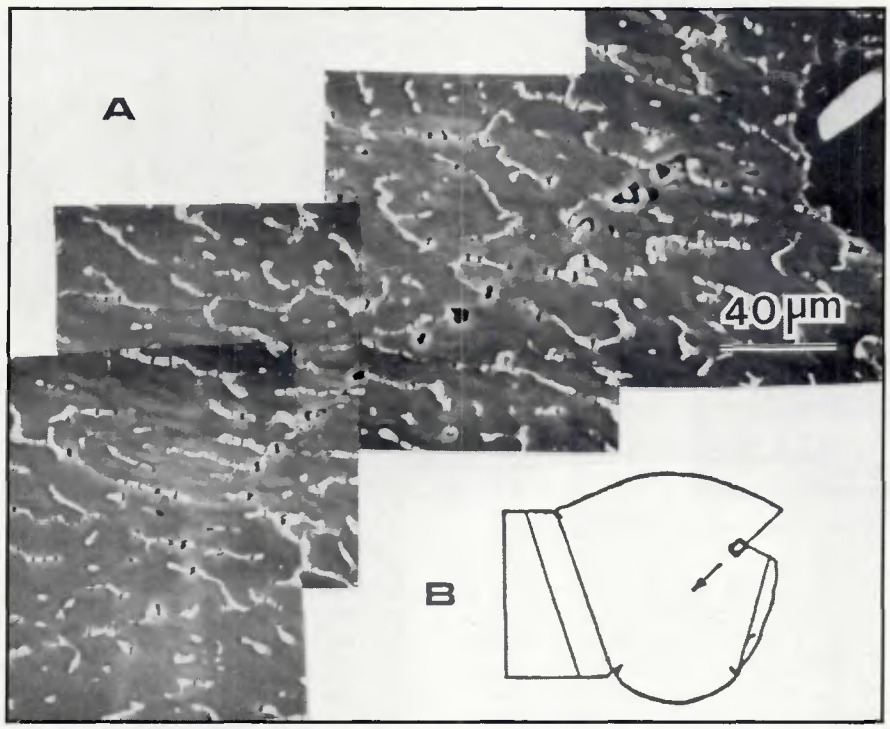

Fig. 19—Series of microvoids initiated at second phase particles in specimen B1P2. A—The line of voids begins at the crack tip (where the fracture path abruptly changes course), and continues towards the diagonally opposite root corner, lying within the proposed crossover regions; B—Schematic of B1P2 showing location and direction of microvoids

are similar to the CRC regions observed here. He suggests the transport of solute to the overlap region (weld corners) involves solute vaporization from the arc-spot region of the weld pool, followed by solute vapor condensation on the surrounding cooler surfaces, including the weld pool surface outside of the arc-spot region and the overlap melt surface. The relatively low boiling points of Mg (2030°F/1110°C) and Zn (1663°F/906°C), compared with Al (4442°F/2450°F), are consistent with the idea that Mg preferentially vaporizes from an Al-Mg system and Zn from an Al-Zn or Al-Zn-Mg system, producing the Mg-rich β structure in the 5456 alloy overlap, and the Zn-rich structure in the X7006 overlap and in the 6061 alloy weld specimen welded with an Al-Zn-Mg wire (Ref. 6). However, the preferential vaporization and condensation of solute is not a likely explanation of the copper-rich θ phase, because copper has a higher boiling point (4703°F/2595°C) than does aluminum (Ref. 8).

Researchers at Vanderbilt University are presently studying the variation of copper content in the fusion zone, particularly in the toe regions, as a function of distance along the weld bead. Hopefully, this will contribute to an understanding of the mechanism causing copper segregation in 2219-T87 aluminum fusion welds.

Conclusions

1. Tensile specimens of VPPA welds of 2219-T87 aluminum plate fail on the rising portion of the stress-strain curve by fracturing prior to necking. The ultimate tensile strength therefore depends on both the flow strength and the ductility (percent elongation of a 2-in. (51-mm)-gauge section). A one percentage point increase in the ductility increases the ultimate tensile strength about 2000 psi.

2. Multiple passes increase the flow strength of VPPA welds.

3. The ultimate tensile strengths of the welds do not go hand-in-hand with the flow strengths because of the separate contribution of the ductility. The ultimate tensile strength of the triple pass weld was nearly matched by the lower-flow-strength double pass condition because

Table 7—Statistical Analysis of Fracture Strength for CRC Structure Removal Study

Weld Type	Weld Category	Specimen Numbers	Average Fracture Strength—AFS (ksi)	Standard Deviation—σ (ksi)	AFS + σ / AFS − σ (ksi)	AFS + 2 σ / AFS − 2 σ (ksi)	AFS + 3 σ / AFS − 3 σ (ksi)
VPPA single pass as-received	B1P	4,6,8,15	39.1	0.82	39.9 / 38.3	40.7 / 37.4	41.5 / 36.6
VPPA single pass cellular structure removed	B1P	3,5,7,9	42.0	0.39	42.4 / 41.7	42.8 / 41.3	43.2 / 40.9
VPPA double pass as-received	B2P	4,6,8,15	41.1	0.68	41.8 / 40.4	42.5 / 39.8	43.2 / 39.1
VPPA double pass cellular structure removed	B2P	3,5,7,9	42.2	0.72	43.0 / 41.5	43.7 / 40.8	44.4 / 40.0
VPPA triple pass as-received	B3P	4,6,8,15	41.8	0.50	42.3 / 41.3	42.8 / 40.8	43.3 / 40.3
VPPA triple pass cellular structure removed	B3P	3,5,7,9	43.6	0.71	44.3 / 42.9	45.1 / 42.2	45.8 / 41.5

Table 8—Summary of Flow Stress, Ductility and Ultimate Tensile Strength Values, B Series (All Welds are Double Pass VPPA Welds with 2319 Filler)

Weld Category	Specimen Numbers	Cellular Structure	Flow Stress at 3.5% Plastic Strain (psi)	Ductility % (From Stress-Strain Curves)	Ultimate Tensile Strength (psi)
B1P	4,6,8,15	intact	38800	~ 3.5	39100
B1P	3,5,7,9	removed	40000	~ 4.6	42000
B2P	4,6,8,15	intact	41400	~ 3.5	41100
B2P	3,5,7,9	removed	42500	~ 3.5	42200
B3P	4,6,8,15	intact	41600	~ 3.3	41800
B3P	3,5,7,9	removed	43400	~ 3.75	43600

of the higher ductility of the double pass weld.

4. Local strain measurements show that the peak strains are produced at the weld corners. This corresponds with the interlayer theory that the majority of plastic flow is confined to diagonal paths across the weld metals.

5. The ductility of the welds is limited by a shallow, brittle, copper-rich cellular (CRC) structure that has unusually high copper content (30–35 wt-% copper), and large volumes of continuous eutectic constituent. This structure is located at the crown and root corners and extends from the surface to depths of 0.001 to 0.003 in. (0.025 to 0.076 mm). Removing the CRC structure increases ultimate strength and ductility values. In the case of the single pass VPPA weld, the removal of the brittle material (thereby reducing the cross-section) actually increased the load carrying capacity.

6. In addition to hardening the first pass, a second pass may serve to relocate the brittle CRC region in a less sensitive location relative to the highly strained crossover regions.

Acknowledgments

The authors wish to thank the Martin Marietta Corporation and NASA/MSFC, which supported this work. They also wish to express their gratitude for the invaluable guidance and logistical support provided by Lynda Johnston, Martin Marietta Corporation, and for the technical advice and valuable discussion offered by Dr. Arthur C. Nunes, Jr., NASA/MSFC. They also acknowledge Mrs. C. Thompson's contribution to the manuscript.

References

1. Nunes, A. C., Jr., Novak, H. L., and McIlwain, M. C. March 1981. Weld geometry strength effect in 2219-T87 aluminum. *NASA Technical Memorandum,* NASA TM-82404.

2. Burghard, H. C., Jr., and Norris, E. G. May 1966. Development of welding techniques and filler metals for high-strength aluminum alloys. Final Report, *NASA Contract NAS8-1529 and NAS8-20160,* Southwest Research Institute.

3. Beil, R. J., and Hahn, G. T. 1983. The influence of weld process variables on crack initiation and growth in 2219-T87 aluminum TIG and VPPA weldments. Final Report, *Martin Marietta Contract No. AS3-756222,* Vanderbilt University, Nashville, Tenn.

4. Beil, R., Hartman, J., and Hahn, G. T. December 1984. The influence of weld process variables on crack initiation and growth in 2219-T87 aluminum TIG and VPPA weldments, Final Report, *Martin Marietta Contract No. AS4 756307,* Vanderbilt University, Nashville, Tenn.

5. D'Annessa, A. T. 1966. Mechanism of overlap segregation in aluminum alloy weldments. *Welding Journal* 45(9):427-s to 432-s.

6. Van Dyke, D. M. January 1983. Metallographic comparison of gas tungsten arc welded and plasma arc welded 2219-T87 aluminum. *Internal Report ETTR 150,* Martin Marietta Corporation.

7. Hartman, J. 1985. Effect of copper-rich regions on tensile properties of TIG and VPPA weldments of 2219-T87 aluminum. Master's Thesis, Vanderbilt University, Nashville, Tenn.

8. *Metals Handbook Desk Edition.* 1985. ASM, Metals Park, Ohio, pp. 6.22–6.25.

WRC Bulletin 318
September 1986

The primary objective of this Bulletin, which contains two papers, is to present a comprehensive picture of the research work conducted to establish the current techniques and procedures for specifying the ferrite content of austenitic stainless steel weld metal and measuring its level.

Factors Influencing the Measurement of Ferrite Content in Austenitic Stainless Steel Weld Metal Using Magnetic Instruments

By E. W. Pickering, E. S. Robitz and D. M. Vandergriff

This report describes a program conducted under the auspices of the Welding Research Council (WRC) Subcommittee on Welding Stainless Steel to identify the optimum procedure for the preparation of austenitic stainless steel weld samples for Ferrite Number (FN) determination.

Measurement of Ferrite Content in Austenitic Stainless Steel Weld Metal Giving Internationally Reproducible Results

By E. Stalmasek

This report is a summary of the results of 14 years' work by the IIW Commission 2 in the field of ferrite content measurement, done prior to 1978.

The publication of these reports was sponsored by the Subcommittee on Welding Stainless Steel of the High Alloys Committee of the Welding Research Council. The price of WRC Bulletin 318 is $24.00 per copy, plus $5.00 for postage and handling. Orders should be sent with payment to the Welding Research Council, Suite 1301, 345 E. 47th St., New York, NY 10017.